ECS | The Electrochemical Society
Advancing solid state & electrochemical science & technology

Improved Particle Swarm Optimization-Extreme Learning Machine Modeling Strategies for the Accurate Lithium-ion Battery State of Health Estimation and High-adaptability Remaining Useful Life Prediction

View the article online for updates and enhancements.

You may also like

CrossMark

Improved Particle Swarm Optimization-Extreme Learning Machine Modeling Strategies for the Accurate Lithium-ion Battery State of Health Estimation and High-adaptability Remaining Useful Life Prediction

Chu-yan Zhang,[1,z] 🔍 Shun-li Wang,[1,2] Chun-mei Yu,[1,2] Yan-xin Xie,[1] and Carlos Fernandez[3]

[1]*School of Information Engineering, Southwest University of Science and Technology, Mianyang 621010, People's Republic of China*
[2]*College of Electrical Engineering, Sichuan University, Chengdu 610065, People's Republic of China*
[3]*School of Pharmacy and Life Sciences, Robert Gordon University, Aberdeen AB10-7GJ, United Kingdom*

To ensure the secure and stable operation of lithium-ion batteries, the state of health (SOH) and the remaining useful life (RUL) are the critical state parameters of lithium-ion batteries, which need to be estimated precisely. A joint SOH and RUL estimation approach based on an improved Particle Swarm Optimization Extreme Learning Machine (PSO-ELM) is proposed in this paper. The approach adopts Pearson coefficients to screen multivariate information of the discharge process as health indicators and uses them as inputs to enable accurate estimation of SOH and RUL prediction of lithium-ion batteries on the basis of the PSO-ELM model. The validity of the model is demonstrated by the NASA lithium-ion battery data set: the maximum root mean square error (RMSE) of the SOH estimation of the tested battery is 0.0033, the maximum RMSE of its RUL prediction is 0.0082, and the maximum absolute error of RUL prediction is one cycle number. In comparison with the prediction results of the traditional extreme learning machine, the optimized model proposed in this paper estimates the SOH of lithium-ion batteries and RUL with relatively high accuracy.
© 2022 The Electrochemical Society ("ECS"). Published on behalf of ECS by IOP Publishing Limited. [DOI: 10.1149/1945-7111/ac8a1a]

The role of security of energy and protection of the environment is decisive in China's expansion program.[1] In all countries, new sources of energy to switch from classical fossil fuels have emerged as the focus of attention.[2] With the benefits of high energy density, high output capacity, and high performance-to-price ratio, lithium-ion batteries have been broadly applied and promoted in the area of renewable energy.[3] Application of which allowed the construction of utility electric vehicles as well as satisfying a number of stringent milestones for electric vehicle economy in regards to energy density, lifetime, security, performance and expense.[4] However, the potential for battery pack fires[5] and combustion cannot be completely eliminated.[6] Hence, a coherent and well-supported lithium-ion battery management system[7] assumes a central function for the security and proper use of lithium-ion batteries.

State of health (SOH) is a quantitative indicator used to assess the extent of battery degradation.[8] As a general rule, SOH is defined as the ratio of the actual remaining capacity of the battery to the rated capacity of the battery.[9] An exact estimate of the state of charge (SOC) of a lithium-ion battery hinges on an accurate estimate of the SOH of the lithium-ion batteries.[10] Furthermore, aging batteries are more prone to thermal runaway.[11] Therefore, it is vital to evaluate reliable methods and strategies to accurately estimate the current remaining capacity and SOH of a battery. What follows are the approaches for estimating the SOH of lithium-ion batteries at this moment.[12]

The characteristic approach is based on the evolution of the characteristic parameters shown during the degradation of the battery,[13] a mapping relationship between the characteristic quantity and the SOH of the battery is constructed, as a result, the SOH is then estimated. The internal resistance approach utilizes the internal resistance of the battery as the chief indicator of battery life.[14] The internal resistance of the battery grows gradually as the battery ages and its capacity reduces.[15] The hardship of SOH estimation by the internal resistance approach is to extract the mapping relationship between SOH and internal resistance, in particular by considering SOC, temperature and multiplicity.[16] Furthermore, the extracted characteristic relationship is only available for a certain brand and model of battery and is by no means very widespread.[17]

Electrochemical impedance spectrum (EIS) analysis is to evaluate the impedance spectrum at different phases of battery aging first, then connect the EIS curve with the equivalent circuit model parameters of the battery, and then locate the SOH on the basis of the relationship between the model parameters and SOH.[18] However, the EIS measurement approach is complicated,[19] which requires special instruments and can only be applied off-line; in addition, similar to the internal resistance approach, the EIS approach shows poor generality which is only applicable to the battery production, design and technological improvement process,[20] which is not applicable to the operational power system. It consists of variance analysis approach and incremental capacity (IC)[21] or incremental voltage (IV) approach.[22]

The modeling approaches[23] consist mainly of the aging mechanism model: analyzing the physical and electrochemical processes inside the battery at the microscopic level, which focuses on the degradation process of the battery. The approach classified as destructive is to disassemble the lithium-ion batteries[24] with diverse aging degrees, obtain samples of the internal materials of the batteries, analyze the correlation between the aging parameters and the remaining capacity of the batteries, and extract the aging mechanism from the massive data obtained, and establish an objective and genuine aging model of lithium-ion batteries by integrating the data.

In addition, the non-destructive approach firstly discovers proper characterization parameters of aging degree and builds the correspondence between these parameters and the aging degree of the battery, thereby deriving the deterioration mechanism model.[25] This approach is similar to the characterization approach, but the accuracy of its SOH estimation is lower than that of the destructive approach, however, the workload is minor, and it is one of the mainstream development directions for the moment, and the technical problem lies in the positioning and acquisition of the characterization parameters.[26]

Adopting the probabilistic modeling approach is to combine the battery equivalent circuit model with probabilistic analysis methods to describe the aging and capacity fading process of the battery, as well as to validate the model experimentally.[27] Alternatively, a probabilistic monotonic echo state network algorithm is used to follow the nonlinear battery aging process on the basis of the time interval associated with the sequence of voltage declines during

[z]E-mail: zcy73741999@163.com

battery capacity and discharge.[28] Benefits of this approach are that only a portion of the battery charge/discharge test is required for SOH estimation;[29] as well as being comparatively simple and accessible to implement,[30] although the extraction of feature maps requires consideration of various elements and extensive workload.[31]

Data-driven based approaches take battery test data as the initial sample, withdraw the evolution law of battery performance during battery degradation by some mechanisms, and then utilize this regularity for SOH estimation.[32] These approaches cover: autoregressive (AR) models, neural networks, support vector machines (SVM), as well as Gaussian process regression.[33–36] The virtues of AR are low computational effort and low complexity, but the demerits are that the accuracy of the outcomes decreases over time.[37] The drawbacks of NN are that vast amounts of comprehensive sample data are requested.[38] The battery side reactions will contribute to the performance degradation of the battery,[39] which is macroscopically manifested as capacity decline and internal resistance enhancement, thus degrading the lifetime of the battery.[40] Precise prediction of the remaining useful life of lithium-ion batteries under various usage situations can not only guarantee the secure and reliable operation of the system,[41] but also maximize the utilization of the remaining value of the batteries.[42] In accordance with the newly researched progress of battery RUL prediction, a unified category of RUL approaches is defined.[43] (1) Model-based prediction approaches, which are characterized by the fact that the RUL forecast model building is only for a certain specific system.[44] (2) Data-driven forecasting approaches: Based on the theory of statistics and machine learning, the forecasting models are constructed directly using historical data. Data-driven models are more vulnerable to be applied to a wide range of situations.[45] (3) Fusion-based approaches: Combine models with data-driven methods and exploit their respective virtues.[46]

Extreme Learning Machine is a novel algorithm to be used in one-layer hidden feedforward neural networks.[47] Drawbacks in comparison to conventional feedforward neural networks. The ELM algorithm produces the connected weights of the input and hidden layers in a random manner, with problems involving slow training velocity, the tendency to fall back into local minima, and learning rate selection sensitivity[48] and the thresholds of the hidden layer neurons, without adjusting them while in training, simply adjust the quantity of hidden layer neurons to derive the unique optimal result.[49] The ELM approach offers rapid learning velocity and excellent generalization properties when compared to traditional training methods.[50]

To more precisely represent the dynamic characteristics of the battery and an attempt to evaluate the battery state, an improved PSO-ELM model is proposed to estimate the SOH and RUL predictions of lithium-ion batteries, and Pearson coefficients are used to filter the health indicators as inputs to the model and the capacity as the output of the model. To affirm the feasibility of the algorithm, a dataset of NASA lithium-ion batteries is used for validation.

Theoretical Analysis

Extreme learning machine.—Extreme learning machines are applied to the output prediction of complex nonlinear systems. Its advantages in terms of fewer training factors, quicker learning and better generalization capabilities. A three-layer structure made up of an import layer, a hidden layer, and an export layer that operates on a stochastic basis is used for the Extreme Learning Machine. Thresholds for the connection weights drawn from the import layer to the hidden layer and for those neurons in the hidden layer are generated at random over the course of the operation. The structure is shown in Fig. 1, instead, the procedure is as follows.
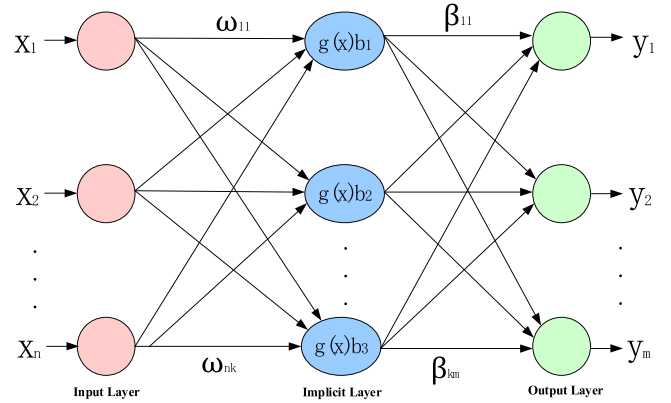

Figure 1. Structure of ELM network.

Assuming that there are N different sample training sets:

$$E = \{(x_p, y_p) | p = 1, 2, \cdots, N, x_p \in R^n, y_p \in R^m\} \qquad [1]$$

In Eq. 1: $x_p \in R^n$, is an input variable of n-dimensional size; $y_p \in R^m$, as the proper export destination vector. If the ELM hidden layer has k amounts of neurons, Then when the input specimen is x_p, the corresponding practical output of the ELM can be expressed as:

$$Y = \sum_{i=1}^{k} \beta_i g(\omega_i \cdot x_i + b_i) i = 1, 2, \cdots, N \qquad [2]$$

In Eq. 2: $\omega_i = (\omega_{1i}, \omega_{2i}, \cdots, \omega_{ni})$ refers to the linkage weights between the first hidden layer neuron and respective cells in the import layer; b_i refers to the ith hidden layer neuron's value of the threshold; $g(\omega_i \cdot x_i + b_i)$ is that the function of activation; $\beta_i = (\beta_{i1}, \beta_{i2}, \cdots, \beta_{im})^T$ refers to the conjunction weight of the first hidden layer neuron of a unit corresponding to the output layer.

The objective of training the ELM network is to resolve the conjunction weights of the hidden layer's mental elements relative to the units in the output layer. While the function of activation $g(x)$ is endlessly separable, the output of the ELM can be represented as:

$$H\beta = Y' \qquad [3]$$

In Eq. 3, $Y' = (y_1, y_2, \cdots, y_N)$ is a linear system of equations consisting of N equations; $\beta = (\beta_1, \beta_2, \cdots, \beta_K)^T$, is the matrix of output weights; H is the hidden layer's output matrix, represented by Eq. 4.

$$H = \begin{pmatrix} g(\omega_i \cdot x_1 + b_1) & \cdots & g(\omega_k \cdot x_k + b_k) \\ \vdots & \ddots & \vdots \\ g(\omega_i \cdot x_N + b_1) & \cdots & g(\omega_k \cdot x_N + b_k) \end{pmatrix} \qquad [4]$$

In contrast, in the context of the ELM algorithm, which is used in the hidden layer, the output matrix H is uniquely determined for the hidden layer as long as the input weights ω_i and the bias b_i are stochastically determined. A one-hidden layer neural network which allows the solution to be trained as a linear system $H\beta = Y'$, where the output weight β that can be determined:

$$\beta = H^+ Y' \qquad [5]$$

In Eq. 5, the generalized inverse matrix H of H^+.

As the conjunction weights for the ELM input and hidden layers and the hidden layer thresholds can be set at random, there is no need to adjust them after they have been set. The connection weights β between the hidden and output layers do not require iterative adjustment, but are determined by addressing the system of equations once. Simply setting the quantity of neurons in the hidden

layers allow you to use the ELM algorithm in order to obtain better output.

Particle swarm optimization algorithm.—Particle Swarm Optimization (PSO) is a computational technique for evolution. It is rooted in the study of birds' behaviour in eating, and the fundamental concept of PSO consists in finding the best solution through cooperation and information sharing within a group of individuals. The bird is abstracted as a particle (point) with no mass or size, and extended up to space in N dimensions.

The particle i's location in space of N dimensions is represented by the vector $x_i = (x_1, x_2, \cdots, x_N)$ and the velocity of flight is represented by the vector $v_i = (v_1, v_2, \cdots, v_N)$. For every particle there is a feasibility value which is derived from the objective function and aware of the best position it so far found (*pbest*) and the position it is now at x_i. In addition this can be considered as the experience of the flight that the particle itself has. Furthermore, every particle is also aware of the best position (*gbest*) that all particles in the whole group have found up to now (*gbest* is the best value in *pbest*), that can be considered as the companion particle's experience. It is by means of its own experience and the companion's best experience that the particle determines its next movement.

The PSO is initialized as a set of stochastic particles. The best available solution is then discovered by iteration. In every iteration, the particles renew themselves through keeping track of two "extremes" (*pbest*, *gbest*). After these two optimal values have been found, the particle renews its speed and location with the use of Eqs. 6 and 7.

$$v_i = v_i + c_1 \times rand() \times (pdest - x_i) \\ + c_2 \times rand() \times (gdest - x_i) \quad [6]$$

$$x_i = x_i + v_i \quad [7]$$

Equations 6 and 7 show that $i = 1,2,\ldots,n$, n which as a total of the particles in this ensemble; v_i which is the particles' velocity; $rand()$ which is a stochastic number in the range of (0, 1); x_i which is the particles' current position; c_1 and c_2 which are learning factors; and v_i whose maximum value is v_{max}, if $v_i > v_{max}$, then $v_i = v_{max}$.

$$v_i = \omega \times v_i + c_1 \times rand() \times (pdest_i - x_i) \\ + c_2 \times rand() \times (gbest_i - x_i) \quad [8]$$

In Eq. 8, ω is the coefficient of inertia with a non-negative value. In case the value is large, the ability to search globally is high while the ability to search locally is weak; in case the value is small, the ability to search globally is weak while the ability to search locally is high. A dynamic ω allows for better search outcomes than a fixed value. The strategy most frequently used is linearly decreasing weights (LDW).

$$\omega^{(t)} = \frac{(\omega_{ini} - \omega_{end})(G_k - g)}{G_k} + \omega_{end} \quad [9]$$

In Eq. 9, G_k shows the maximum number of generations, ω_{ini} shows the primal weights of inertia and ω_{end} that is the inertia weight at the time of iteration to the maximum number of evolved generations. It has improved dramatically with the introduction of ω, and the ability to tune global and local searches for uninterrupted search problems has led to successful applications of the PSO algorithm to a variety of practical problems. Equation 7 as well as Eq. 8 are considered standard PSO algorithms.

The standard PSO algorithm flow is shown in Fig. 2.

1) To initialize a set of particles (population size N), consisting of stochastic positions and velocities.
2) To evaluate every particle's fitness.

3) As for every particle, a comparison is made between its adaptability value and the optimal location *pbest* through which it passes, and in case it is the superior one, then it is taken as the current optimal location *pbest*.
4) As for every particle, a comparison is made between its adaptability value and the optimal position *gbest* through which it passes, and in case it is the superior one, then it is taken as the current optimal location *gbest*.
5) The speed and location of the particles are adjusted based on Eqs. 7 and 8.
6) If the end condition is not accomplished then go to step 2).

PSO-ELM algorithm

The random nature of the ELM initialization parameter generation method leads to the model inevitably generating problems such as redundancy of implied layer neurons and poor identification of unknown input parameters, which reduces the prediction accuracy. Hence, the PSO algorithm in this section is used to find the optimal input weights and hidden layer neurons for ELM and to construct a PSO-ELM model to boost the estimation precision of SOH and RUL. Figure 3 illustrates the flow chart of the PSO-ELM algorithm which is on the basis ofhed assessing the lithium-ion battery.

Following are the detailed steps:

1) The input powers of the ELM and the neuronal thresholds in the hidden layer are encoded as particles, generate the initial populations and initialize them.
2) With the aim of calculating the fitness values for all particles, the mean square error of the ELM network was chosen as the target factor to calculate the PSO fitness values, and its expression is:

$$S_{MSE} = \frac{1}{N} \sum_{i=1}^{N} (T(i) - Y(i))^2 \quad [10]$$

In Eq. 10: N is the sample counts, T is the forecast output for each particle, and Y is the real output of the sample.
3) Search for individual extremes and population extremes of the initial particles based on the fitness values of the initial particles.
4) Optimization is iterative, updating the position and velocity of the particles to get new particles.
5) Determine if the termination condition ($S_{MSE} \leqslant 0.0001$ or the maximum number of iterations is attained) is satisfied. In case it is satisfied, exit to restore the optimal individual, or else skip to step 2) and go on.
6) The end of iterative optimization, decoding the output with the optimal solution.

Lithium-ion battery Health indicators and Correlation analysis

Construction of indirect health index of lithium-ion battery.—It is obvious from the performance of lithium-ion batteries that the physical discharge capacity reflects the battery life state immediately, that is, the direct health factor; while the indirect health factor points to other characteristic parameters that have a relatively strong dependence on the actual discharge capacity of lithium-ion battery and can reflect the degradation state of the battery, which are typically available in charge/discharge voltage, current, temperature and other parameters that can be easily measured and monitored online. In the existing investigations, there exist indirect health factors for lithium-ion batteries in terms of equal voltage drop discharge time, equal time average voltage drop, etc. The approach to forecast the RUL of lithium-ion batteries by utilizing the correlation model between the historical capacity data and the cycle counts of lithium-ion batteries refers to direct prediction; while the indirect prediction means that the RUL of lithium-ion batteries is forecasted by setting up the correlation model between the indirect health factor and the actual degradation capacity. Compared with the
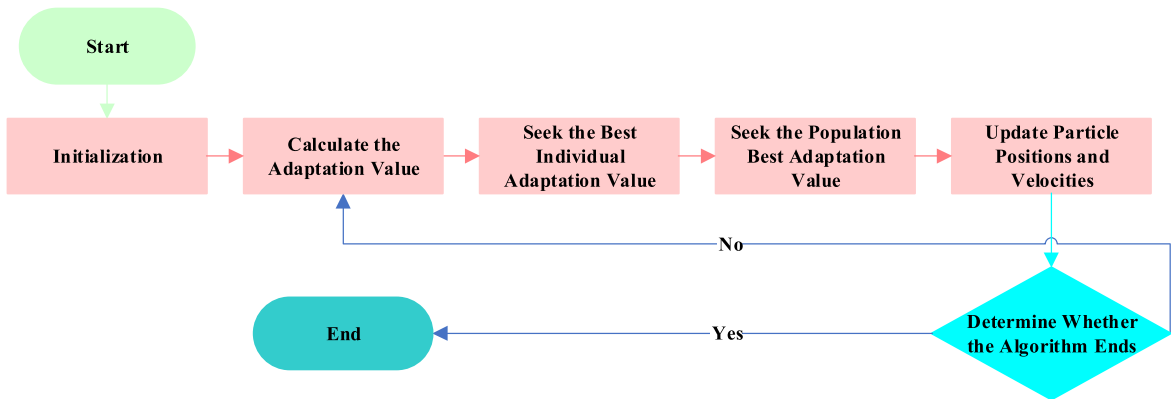
Figure 2. Flow chart of the standard PSO algorithm.
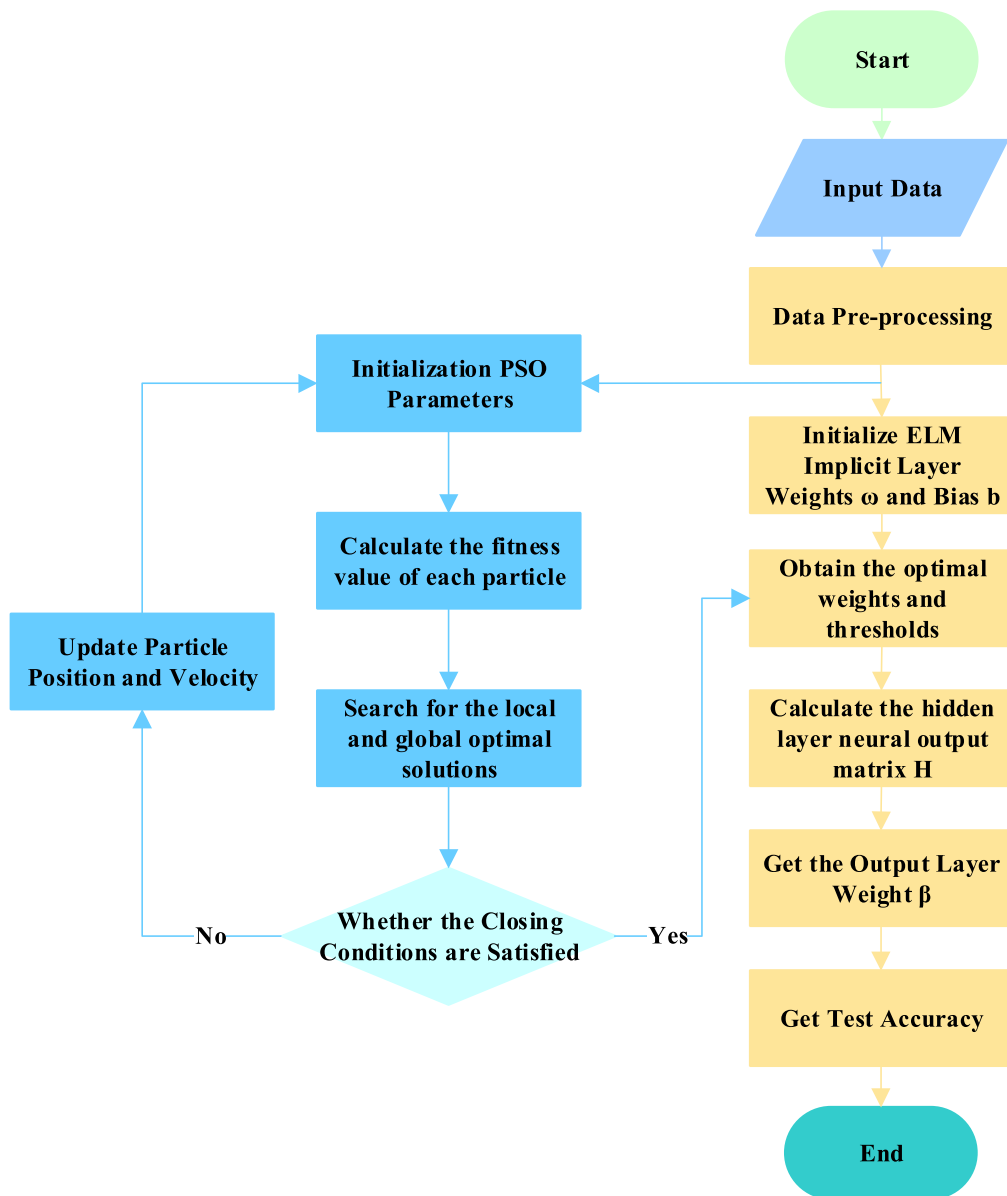
Figure 3. Flowchart of soc estimation based on PSO-ELM.

direct prediction, the indirect prediction method is diverse, general-ized and more flexible.

Health indicators extraction.—Figure 4 reveals the process and framework optimization of the novel health indicators extraction in the following steps:
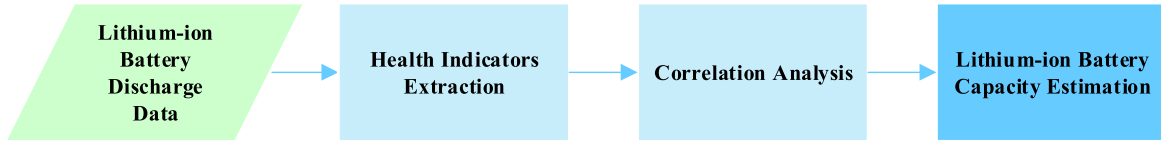
Figure 4. HI extraction framework.

1) Feature extraction (HI extraction): The raw lithium-ion battery discharge data are analyzed to extract the discharge voltage, temperature and other data and screen out the available data as a backup.
2) Correlation analysis: The derived HI and battery capacity are correlated to validate the magnitude of correlation.
3) Lithium-ion battery capacity estimation: The capacity is estimated with the customized new HI and compared with the practical capacity for analysis.

Correlation analysis.—The Pearson coefficient shows the quotient of the covariance of the two variables with their standard deviation, which is represented by p.

$$p_{XY} = \frac{cov(X, Y)}{\sigma_X \sigma_Y} = \frac{E(XY) - E(X)E(Y)}{\sqrt{E(X^2) - E^2(X)}\sqrt{E(Y^2) - E^2(Y)}} \quad [11]$$

In Eq. 11: $cov(X, Y)$ means the covariance of variables X and Y, σ_X, σ_Y denote the standard deviation of variables X, Y and E(X) is the mathematical expectation of X, E(Y) is the mathematical expectation of Y. The absolute value of the global Pearson coefficient is less than or equal to 1. If the absolute value of the correlation coefficient equals to 1, which means that the two variables completely lie on the one line.

Experimental Analysis

Lithium-ion Battery experimental data presentation.—The battery degradation characteristics and approach to validate in this paper adopts the experimental data published by NASA PCoe for lithium-ion battery, whose model is 18650 lithium-ion battery with a nameplate capacity of 2Ah. The data set consists of several sets of experiments, in which each set of experiments performs successive charging and discharging of lithium-ion battery in various conditions, which includes three processes: charging, discharging, and alternating current impedance (EIS) measure the battery impedance. The B5 aging battery pack is selected as the investigation target in this paper. The battery pack experiments are conducted under room temperature conditions, in which charging is performed at a steady current (CC) mode of 1.5 A up to the battery voltage of 4.2 V, and then charging is kept at a steady voltage (CV) mode until the charging current falls to 20 mA. The discharge is performed at a constant current (CC) level of 2 A as long as the battery meets the cut-off voltage and ceases to discharge, and an EIS impedance measurement is performed after each charge and discharge. The battery is subjected to sequential cycles of accelerated degradation until the end of life, which is defined as a 30% decay in the maximum capacity of the battery. The experimental conditions and data recorded for each cycle are shown in Table I and II.

Co-estimation of SOH and RUL for lithium-ion battery.—In this paper, with the NASA battery data as a case study, the co-estimation of the SOH and RUL approach based on PSO-ELM is implemented to filter out the health indicators and constrain the estimated lithium-ion battery SOH and RUL model by correlation analysis of the variables of the experimental data, and the model is constructed and trained by Matlab 2018a based.

Health indicators Extraction.—With the purpose of attaining the precise estimation of lithium-ion battery SOH and RUL, firstly, to extract the health indicators of the lithium-ion battery, the specific data are illustrated in Table III.

Since the tendency of each health indicator is diverse, the correlation between it and capacity cannot be judged straightforwardly. For the purpose of further quantifying the extent of correlation between health indicators and capacity, the Pearson correlation coefficient to measure the correlation between HI and capacity is adopted in this paper.

The two HIs with Pearson coefficients above 0.95 were selected as the inputs to the model in order to ensure that the extracted HIs could be adapted to different conditions. As can be observed in Table IV, the correlation between I1 and I4 and the actual capacity is relatively strong, so the approach of selecting the equal voltage drop discharge time and the number of cycles from the initial to the current lithium-ion battery as indirect health indicators for battery SOH and RUL forecasting possesses correctness and feasibility.

The analysis of SOH and RUL prediction results.—While both SOH and RUL can estimate the battery degradation extent, they both differ in their principles and scope of application. In consideration of the links and distinctions between them, a joint estimation of SOH and RUL based on the PSO-ELM model is proposed in this paper. The HI is extracted from the current, voltage and temperature curves, and the derived HI is used as input and capacity as output to build a PSO-ELM based battery degradation model. Afterwards, the overall variation trend through HI is modeled by PSO-ELM and combined with the established battery aging model for SOH estimation to achieve the battery RUL estimation.

The lithium-ion battery data (B0005) is used in this paper to authenticate the precision and reliability of the PSO-ELM algorithm with a total of 168 cycles of B0005. In addition, the mean absolute error (MAE) and root mean squared error (RMSE) were used as the evaluation metrics for the algorithm performance.

$$RMSE = \sqrt{\frac{1}{N}\left(\sum_{i=1}^{N}(x_i - \hat{x}_i)^2\right)} \quad [12]$$

$$MAE = \frac{1}{N}\sum_{i=1}^{N}|x_i - \hat{x}_i| \quad [13]$$

Results of SOH estimation–With the purpose of investigating the accuracy and stability of the formulated battery aging model, the anterior 60% of the lithium-ion battery data is taken as the training set and the posterior 40% as the test set, which means that the

Table I. NASA dataset battery pack experimental conditions.

Battery	Temperature	Charging Current	Discharging Current	Cut-off Voltage
B5	24 °C	1.5 A	2 A	2.7 V

Table II. NASA dataset experimental data.

Charging Process	Discharge Process	Impedance Measurement
Battery Voltage	Battery Voltage	Induction Current
Battery Current	Battery Current	Battery Current
Load Voltage	Load Voltage	Battery Impedance
Load Current	Load Current	Calibration Impedance
Time	Time	Ohmic Resistance
–	Discharge Power	Charge Transfer Impedance

Table III. Lithium-ion battery health indicators description.

Indicator	Indicator Description	Numerical Range
I1	The time it takes for the discharge voltage to go from 3.8 V to 3.5 V (min)	(13,30)
I2	The average value of battery voltage during discharging	(3.46,3.56)
I3	The average value of battery temperature during discharging	(31.33,34.31)
I4	The cycle times from the start of battery use to the current cycle	(1,168)

Table IV. The Pearson correlation coefficient of HI.

	I1	I2	I3	I4
B0005	0.996	0.954	−0.810	−0.991

anterior 100 cycles of B0005 are the training set and the posterior 68 cycles are the test set. In each cycle, the two selected HIs are extracted from the equal voltage reduction discharge time and the number of cycles curves, and the results are provided as input to the PSO-ELM model to derive the corresponding SOH estimation values. It is observed in Figs. 5 and 6 that the estimated and true values, where SOH1 is the true value, the true value of capacity is measured by discharging a fully charged battery at constant current up to the cutoff voltage, SOH2 is the estimated value of the test set, and SOH3 is the estimated value of the training set, from which it can be seen that the estimated values can not only capture the SOH decline trend of lithium-ion battery properly, but also can be well adapted to the regeneration phenomenon of the aging process, and can get more accurate SOH estimation.

In Figs. 5 and 6, the forecast results of the ELM algorithm for B0005 differ significantly from the actual value; as the algorithm keeps optimizing, the forecast value of the PSO-ELM algorithm is getting closer to the actual value, which means that the forecast accuracy of the lithium-ion battery of the state of health is getting higher and higher.

According to the relative error of the forecast results of the two algorithms shown in Figs. 5 and 6, it is clear that the relative error of

the original ELM algorithm without optimization can exceed 20% in absolute value at each sample point of the test data, and the prediction accuracy cannot reach the requirement; the prediction results after PSO optimization further improve the prediction accuracy of the model, and the relative error with evil can be controlled within 1.5% to achieve the expected effect. Table V lists the MAE and RMSE calculation results, where the B0005 battery based on PSO-ELM algorithm error calculated less than 0.5%. It is further verified that the SOH estimation method proposed in this paper has relatively high precision. While the literature[51] treats the B0007 dataset for training and the B0005 dataset for testing, the RMSE estimated by the parallel layer extreme learning machine (PL-ELM) algorithm is 0.362 after experimental validation. Thus, it can be seen that the SOH estimation method proposed in this paper has higher accuracy, and the former one hundred cycles of data are selected for training in this paper, which shows that the prediction performance of the method is excellent.

Results of RUL estimation–Regarding for B0005, there are 168 cycles of battery capacity data, respectively, the capacity data and cycle data of the former 60 and 70 cycles as offline training data, which means the prediction starting point is as follows: co=60, co=70 cycles, and the end-of-life (EOL) cycle as the 101st, and the data from the prediction starting point to the 168th charge/discharge as the test data. With the RUL prediction outcomes of ELM and PSO-ELM algorithms for the B0005 battery presented in Fig. 7 and 8, where C1 is the true value, C2 is the estimated value of the training set, and C3 is the estimated value of the test set, C4 is the failure capacitance value, respectively, and more intuitively in Table VI, where Fig. 9 shows the RUL prediction errors of both approaches for the battery B0005 at the initial point C0 = 60.

In Table VI, C0 denotes the prediction starting point; RUL_p denotes the battery RUL prediction value; RUL_t denotes the battery true RUL value; the units of the above indicators are: times; RUL_e denotes the absolute error of the RUL prediction value, which is defined as in Eq. 14; RUL_r denotes the relative error of RUL prediction value, which is defined as in Eq. 15:

$$RUL_e = |RUL_p - RUL_t| \qquad [14]$$
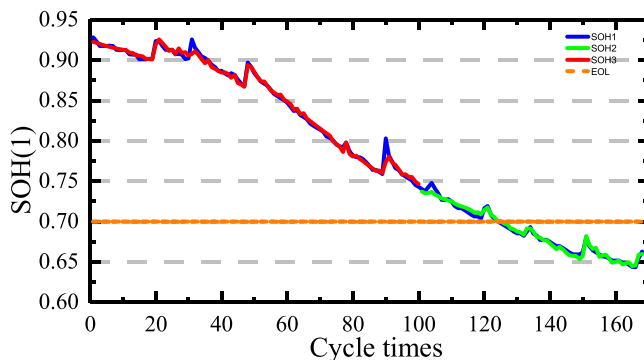
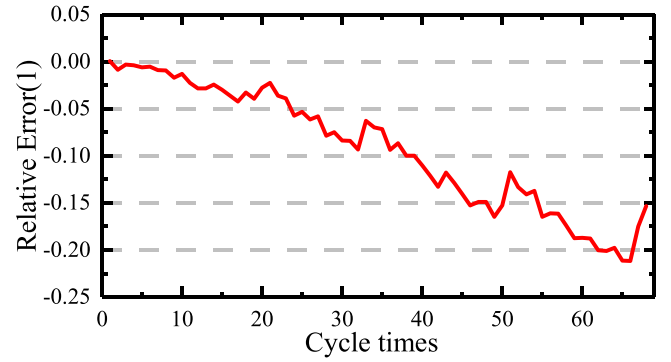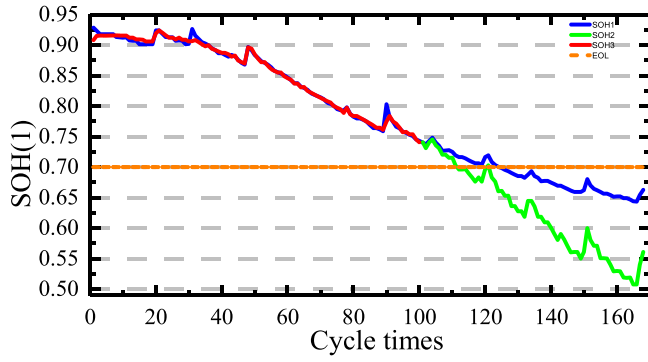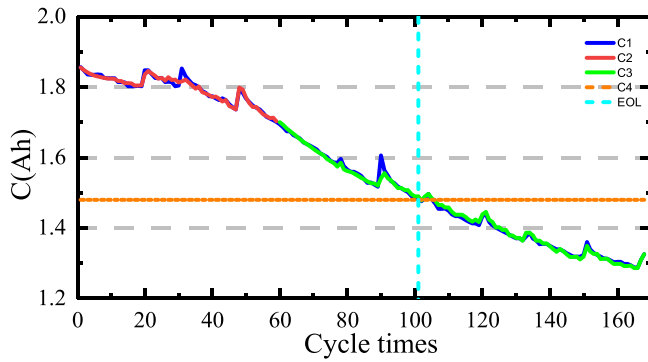**Figure 5.** Results of SOH estimation based on PSO-ELM model.
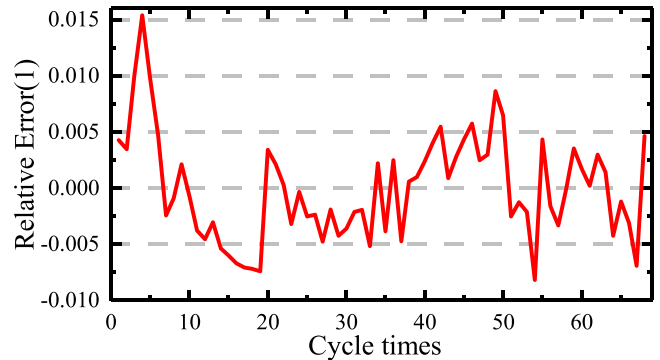
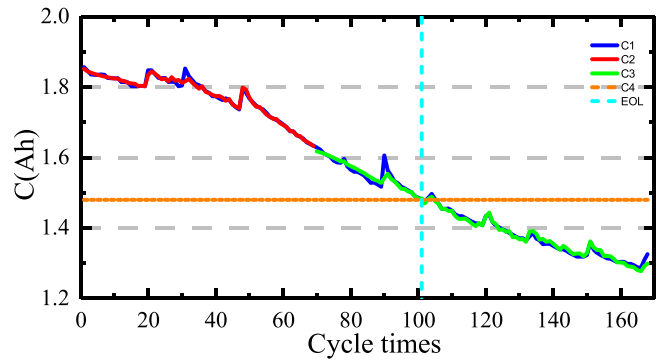**Figure 6.** Results of SOH estimation based on ELM model.

Table V. SOH estimation error results.

Battery	Algorithm	MAE	RMSE
B0005	ELM	0.0269	0.0478
	PSO-ELM	0.0026	0.0033

As can be intuitively observed from Figs. 7–9 and Table VI, in comparison with the ELM algorithm, the PSO-ELM algorithm has superior life prediction performance for the battery B0005, where the prediction curve is relatively close to the actual capacity degradation curve; the PSO-ELM model prediction errors are all within 1 cycles; in addition, by increasing the training data, the prediction errors progressively decline and the prediction perfor-
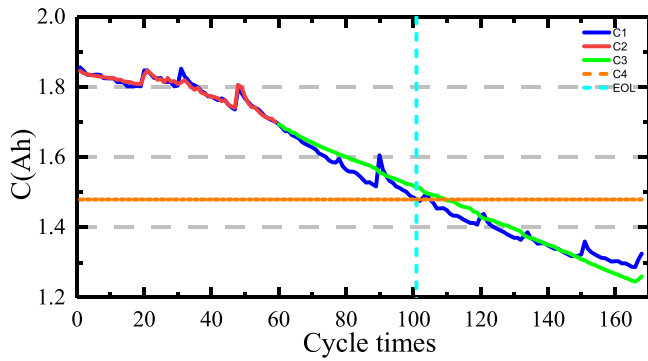

(a) Prediction starting point C0=60

(b) Prediction starting point C0=70

Figure 7. Results of RUL estimation based on PSO-ELM model.

(c)Prediction starting point C0=60
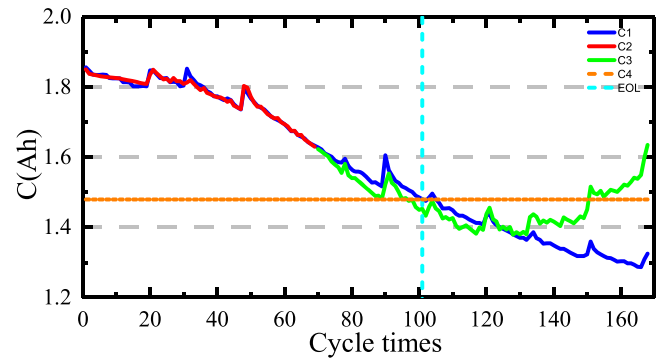
(d) Prediction starting point C0=70

Figure 8. Results of RUL estimation based on ELM model.

$$RUL_r = \frac{|RUL_p - RUL_t|}{RUL_t} \times 100\% \qquad [15]$$

mance becomes better and better, and the absolute error can down to 1 cycles, and more accurate battery RUL estimation is accomplished.

In the case of the prediction point C0=60, the MAE and RMSE of the outcomes estimated by PSO-ELM and ELM algorithms are to be as presented in Table VII.

Table VI. Comparison of the RUL prediction performance of two algorithms for B0005 battery.

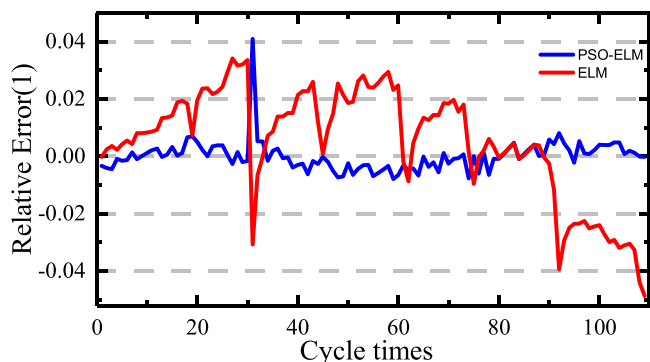|	Algorithm	RUL_p	RUL_t	RUL_e	RUL_r
C0=60	ELM	42	41	1	2.44%
	PSO-ELM	50		9	21.95%
C0=70	ELM	32	31	1	3.23%
	PSO-ELM	37		6	19.35%

Figure 9. Relative error of RUL prediction results.

Table VII. RUL estimation error results.

Battery	Algorithm	MAE	RMSE	MSE
B0005	ELM	0.0236	0.0282	0.00080
	PSO-ELM	0.0049	0.0082	0.00007

It can further be observed from Table VII that compared with the ELM algorithm with unoptimized model parameters, the forecasting errors of the PSO-ELM approach in this paper are narrower, the MAE of the PSO-ELM algorithm is 0.0049, and the MSE of the PSO-ELM algorithm is 0.00007 which can cater to the requirements of lithium-ion battery applications for remaining useful life prediction. Whereas, the literature[52] trains the B0005 dataset for the former 83 cycles and tests the latter 82 cycles, and the MSE estimated by the heuristic Kalman algorithm-multi-layer ELM (HKA-ML-ELM) algorithm is 0.0002 after experimental validation. Thus, it can be seen that the accuracy of the RUL estimation method proposed in this paper is higher, and the accuracy of estimation is greatly improved by extracting health indicators in this paper, which is more conducive to practical application.

Conclusion

An improved SOH estimation and RUL prediction model for lithium-ion batteries with PSO-ELM is proposed in this paper. The multivariate information of voltage, temperature and time of the discharge process is extracted as the characteristic parameters, the Pearson coefficients are used to filter the health indicators, which are used as the inputs of the PSO-ELM model, while capacity is used as the output. The validity of the model was verified based on the NASA lithium-ion battery dataset, and the results demonstrate that the proposed SOH and RUL estimation algorithm has superior accuracy: the maximum RMSE of SOH estimation for the B0005 battery is 0.0033, the maximum RMSE of RUL prediction is 0.0082, and the maximum absolute error of RUL prediction for different prediction starting points are selected for one cycle number. Nevertheless, the method has not been validated under other batteries or more complex operating conditions, and thus needs further optimization. In order to improve the reliability and accuracy

of the health assessment of lithium-ion batteries, future work will be improved from the following three points: (1) Selecting more health indicators that reflect the characteristics of lithium-ion batteries for analysis; (2) Establishing the battery electrochemical model; (3) Implementing a more optimal algorithm to solve the model parameters.

ORCID

Chu-yan Zhang ⓘ https://orcid.org/0000-0001-9200-0734

References

1. X. X. Bi, K. Amine, and J. Lu, "The importance of anode protection towards lithium oxygen batteries." *J. Mater. Chem. A*, **8**, 3563 (2020).
2. M. Segalovich, A. Berl, U. Aviv, E. Jaffe, R. Shelef, J. Haik, M. Cleary, R. Kornhaber, and M. Harats, "The hidden danger of lithium battery-powered electric bicycles and scooters: a case series of the israeli national burn center experience." *Journal of Burn Care & Research*, **43**, 504 (2022).
3. X. Zhang, Y. Han, and W.-P. Zhang, "A review of factors affecting the lifespan of lithium-ion battery and its health estimation methods." *Transactions on Electrical and Electronic Materials*, **22**, 567 (2021).
4. L. Y. Shao, R. Navaratne, M. Popescu, and G. P. Liu, "Design and construction of axial-flux permanent magnet motors for electric propulsion applications-a review." *Ieee Access*, **9**, 158998 (2021).
5. S. Sripad, A. Bills, and V. Viswanathan, "A review of safety considerations for batteries in aircraft with electric propulsion." *MRS Bull.*, **46**, 435 (2021).
6. X. Y. Liu, K. Reddi, A. Elgowainy, H. Lohse-Busch, M. Wang, and N. Rustagi, "Comparison of well-to-wheels energy use and emissions of a hydrogen fuel cell electric vehicle relative to a conventional gasoline-powered internal combustion engine vehicle." *Int. J. Hydrogen Energy*, **45**, 972 (2020).
7. Y. J. Wang, R. L. Xu, C. J. Zhou, X. Kang, and Z. H. Chen, "Digital twin and cloud-side-end collaboration for intelligent battery management system." *J. Manuf. Syst.*, **62**, 124 (2022).
8. S. Park, J. Ahn, T. Kang, S. Park, Y. Kim, I. Cho, and J. Kim, "Review of state-of-the-art battery state estimation technologies for battery management systems of stationary energy storage systems." *Journal of Power Electronics*, **20**, 1526 (2020).
9. Y. J. Wang, J. Q. Tian, Z. D. Sun, L. Wang, R. L. Xu, M. C. Li, and Z. H. Chen, "A comprehensive review of battery modeling and state estimation approaches for advanced battery management systems." *Renewable Sustainable Energy Rev.*, **131**, 1 (2020).
10. X. J. Tan, Y. Q. Tan, D. Zhan, Z. Yu, Y. Q. Fan, J. Z. Qiu, and J. Li, "Real-time state-of-health estimation of lithium-ion batteries based on the equivalent internal resistance." *Ieee Access*, **8**, 56811 (2020).
11. S. Rahimifard, R. Ahmed, and S. Habibi, "Interacting multiple model strategy for electric vehicle batteries state of charge/health/ power estimation." *Ieee Access*, **9**, 109875 (2021).
12. H. Yao, X. Jia, Q. Zhao, Z. J. Cheng, and B. Guo, "Novel lithium-ion battery state-of-health estimation method using a genetic programming model." *Ieee Access*, **8**, 95333 (2020).
13. Y. Y. Jiang, J. Zhang, L. Xia, and Y. B. Liu, "State of health estimation for lithium-ion battery using empirical degradation and error compensation models." *Ieee Access*, **8**, 123858 (2020).
14. P. Ren, S. L. Wang, M. F. He, and W. Cao, "Novel strategy based on improved Kalman filter algorithm for state of health evaluation of hybrid electric vehicles Li-ion batteries during short- and longer term operating conditions." *Journal of Power Electronics*, **21**, 1190 (2021).
15. M. A. Kamali, A. C. Caliwag, and W. Lim, "Novel SOH estimation of lithium-ion batteries for real-time embedded applications." *IEEE Embedded Sys. Lett.*, **13**, 206 (2021).
16. K. Gaouzi, H. El Fadil, A. Rachid, A. Lassioui, Z. El Idrissi, and F. Giri, "Sampled-data observer for estimating the state of charge, state of health, and temperature of batteries." *Electric Power Components and Systems*, **48**, 2168 (2021).
17. L. Chen, Z. Q. Lu, W. L. Lin, J. Z. Li, and H. H. Pan, "A new state-of-health estimation method for lithium-ion batteries through the intrinsic relationship between ohmic internal resistance and capacity." *Measurement*, **116**, 586 (2018).
18. J. B. Li, M. Ye, K. P. Gao, X. X. Xu, M. Wei, and S. J. Jiao, "Joint estimation of state of charge and state of health for lithium-ion battery based on dual adaptive extended Kalman filter." *Int. J. Energy Res.*, **45**, 13307 (2021).
19. T. K. Pradyumna, K. Cho, M. Kim, and W. Choi, "Capacity estimation of lithium-ion batteries using convolutional neural network and impedance spectra." *Journal of Power Electronics*, **22**, 850 (2022).
20. S. Alam et al., "Uphill and downhill charge generation from charge transfer to charge separated states in organic solar cells." *J. Mater. Chem. C*, **9**, 14463 (2021).
21. Q. C. Zhang, X. Li, C. Zhou, Y. Zou, Z. C. Du, M. G. Sun, Y. S. Ouyang, D. Yang, and Q. Q. Liao, "State-of-health estimation of batteries in an energy storage system based on the actual operating parameters." *Journal of Power Sources*, **506**, 230162 (2021).

22. Z. B. Wei, G. Z. Dong, X. A. Zhang, J. Pou, Z. Y. Quan, and H. W. He, "Noise-immune model identification and state-of-charge estimation for lithium-ion battery using bilinear parameterization." *IEEE Trans. Ind. Electron.*, **68**, 312 (2021).

23. P. Venugopal, S. S. Shankar, C. P. Jebakumar, R. Agarwal, H. H. Alhelou, S. S. Reka, and M. E. H. Golshan, "Analysis of Optimal Machine Learning Approach for Battery Life Estimation of Li-Ion Cell." *Ieee Access*, **9**, 159616 (2021).

24. Y. Z. Cui, P. J. Zuo, C. Y. Du, Y. Z. Gao, J. Yang, X. Q. Cheng, Y. L. Ma, and G. P. Yin, "State of health diagnosis model for lithium ion batteries based on real-time impedance and open circuit voltage parameters identification method." *Energy*, **144**, 647 (2018).

25. C. Jin, S. Gao, S. Sun, and C. Tian, "Analysis of safety performance of lithium-ion power battery during life cycle based on non-destructive testing." *Energy Storage Science and Technology*, **8**, 259–63 (2019).

26. K. Qian, B. H. Huang, A. H. Ran, Y. B. He, B. H. Li, and F. Y. Kang, "State-of-health (SOH) evaluation on lithium-ion battery by simulating the voltage relaxation curves." *Electrochim. Acta*, **303**, 183 (2019).

27. Q. Huo, Z. K. Ma, X. S. Zhao, T. Zhang, and Y. L. Zhang, "Bayesian network based state-of-health estimation for battery on electric vehicle application and its validation through real-world data." *Ieee Access*, **9**, 11328 (2021).

28. J. F. Jia, K. K. Wang, X. Q. Pang, Y. H. Shi, J. Wen, and J. C. Zeng, "Multi-scale prediction of RUL and SOH for lithium-ion batteries based on WNN-UPF combined model." *Chin. J. Electron.*, **30**, 26 (2021).

29. A. Sorour, M. Fazeli, M. Monfared, A. A. Fahmy, J. R. Searle, and R. P. Lewis, "Forecast-based energy management for domestic pv-battery systems: a UK case study." *Ieee Access*, **9**, 58953 (2021).

30. T. A. Woodruff, J. DiFrancesco, M. Kurth, A. Marinelli, and K. M. Cienkowski, "Disposable hearing aid battery management: survey assessment of providers and qualitative interviews of patients." *American Journal of Audiology*, **30**, 730 (2021).

31. J. Li, Q. Zhou, Y. L. He, H. Williams, and H. M. Xu, "Driver-identified supervisory control system of hybrid electric vehicles based on spectrum-guided Fuzzy feature extraction." *IEEE Trans. Fuzzy Syst.*, **28**, 2691 (2020).

32. S. Z. Zhang, X. Guo, and X. W. Zhang, "Multi-objective decision analysis for data-driven based estimation of battery states: a case study of remaining useful life estimation." *Int. J. Hydrogen Energy*, **45**, 14156 (2020).

33. F. Liu, Y. P. Liu, W. X. Su, C. P. Jiao, and Y. Liu, "Online estimation of lithium-ion batteries state of health during discharge." *Int. J. Energy Res.*, **45**, 10112 (2021).

34. J. Kim, H. Chun, M. Kim, J. Yu, K. Kim, T. Kim, and S. Han, "Data-driven state of health estimation of li-ion batteries With RPT-reduced experimental data." *Ieee Access*, **7**, 106986 (2019).

35. N. Shateri, D. J. Auger, A. Fotouhi, and J. Brighton, "An experimental study on prototype lithium-sulfur cells for aging analysis and state-of-health estimation." *Ieee Transactions on Transportation Electrification*, **7**, 1324 (2021).

36. X. S. Hu, Y. H. Che, X. K. Lin, and Z. W. Deng, "Health prognosis for electric vehicle battery packs: a data-driven approach." *Ieee-Asme Transactions on Mechatronics*, **25**, 2622 (2020).

37. M. Tripathi, M. M. Sucheendran, and A. Misra, "Effect of aspect ratio variation on subsonic aerodynamics of cascade type grid fin at different gap-to-chord ratios." *Aeronaut. J.*, **124**, 472 (2020).

38. M. Ali, M. Adnan, M. Tariq, and H. V. Poor, "Load forecasting through estimated parametrized based fuzzy inference system in smart grids." *IEEE Trans. Fuzzy Syst.*, **29**, 156 (2021).

39. Y. J. Wang, L. Wang, M. C. Li, and Z. H. Chen, "A review of key issues for control and management in battery and ultra-capacitor hybrid energy storage systems." *Etransportation*, **4**, 1 (2020).

40. Y. H. Wang, L. Hao, and M. L. Bai, "Effect of CO_2-induced side reactions on the deposition in the non-aqueous Li-air batteries." *J. Solid State Electrochem.*, **25**, 2571 (2021).

41. L. Chen, H. M. Wang, J. Chen, J. J. An, B. Ji, Z. Q. Lyu, W. P. Cao, and H. H. Pan, "A novel remaining useful life prediction framework for lithium-ion battery using grey model and particle filtering." *Int. J. Energy Res.*, **44**, 7435 (2020).

42. L. Chen, J. Chen, H. M. Wang, Y. J. Wang, J. J. An, R. Yang, and H. H. Pan, "Remaining useful life prediction of battery using a novel indicator and framework with fractional grey model and unscented particle filter." *IEEE Trans. Power Electron.*, **35**, 5850 (2020).

43. A. El Mejdoubi, H. Chaoui, J. Sabor, and H. Gualous, "Remaining useful life prognosis of supercapacitors under temperature and voltage aging conditions." *IEEE Trans. Ind. Electron.*, **65**, 4357 (2018).

44. Y. Lei, N. Li, S. Gontarz, J. Lin, S. Radkowski, and J. Dybala, "A model-based method for remaining useful life prediction of machinery." *IEEE Trans. Reliab.*, **65**, 1314 (2016).

45. K. Liu, Y. Shang, Q. Ouyang, and W. D. Widanage, "A data-driven approach with uncertainty quantification for predicting future capacities and remaining useful life of lithium-ion battery." *IEEE Trans. Ind. Electron.*, **68**, 3170 (2020).

46. U. E. Akpudo and J.-W. Hur, "A feature fusion-based prognostics approach for rolling element bearings." *J. Mech. Sci. Technol.*, **34**, 4025 (2020).

47. H. T. Wong, H. C. Leung, C. S. Leung, and E. Wong, "Noise/fault aware regularization for incremental learning in extreme learning machines." *Neurocomputing*, **486**, 200 (2022).

48. R. Xu, X. Liang, Y. Ma, and J. Qi, "Adaptive Orthogonal Search for Network Structure Learning of ELM." *Chin. J. Comput.*, **44**, 1888 (2021).

49. Q. Wang, M. Wei, M. Ye, J. Li, and X. Xu, "Estimation of lithium-ion battery SOC based on GWO-optimized extreme learning machine." *Energy Storage Science and Technology*, **10**, 744 (2021).

50. M. S. H. Lipu, M. A. Hannan, A. Hussain, M. H. Saad, A. Ayob, and M. N. Uddin, "Extreme learning machine model for state-of-charge estimation of lithium-ion battery using gravitational search algorithm." *IEEE Trans. Ind. Appl.*, **55**, 4225 (2019).

51. E. Ezemobi, A. Tonoli, and M. Silvagni, "Battery state of health estimation with improved generalization using parallel layer extreme learning machine." *Energies*, **14**, 1 (2021).

52. Y. Y. Ma, D. X. Shen, L. F. Wu, Y. Guan, and H. Zhu, "The remaining useful life estimation of lithium-ion batteries based on the HKA -ML-ELM algorithm." *Int. J. Electrochem. Sci.*, **14**, 7737 (2019).